CHAPTER 4-Mechanistic effects of AgENPs

INTRODUCTION

Bivalves, particularly mussels, are widely used to monitor environmental change, particularly in relation to the presence of contaminants. This explains the availability of the sequences of certain genes involved in stress response and to pollutants (Barsyte et al., 1999; Yang HL et al., 2004).

Molluscs can absorb the metals compound both from dissolved like ions the water than like suspended particles. In general, the absorption process is cell-specific and metal-specific. Soluble metal species and the free metal ions are more bioavailable and more toxic than the insoluble forms of the same metals, although a greater hydrophobicity often results in a greater tendency of the compound to partition and persist in the tissues of the organism (Widdows and Donkin, 1992).

Mussels, including *Mytilus galloprovincialis*, are well studied at the molecular, cellular, tissue, and organismal levels. These filter-feeding organisms are usually used in large monitoring programs to evaluate the accumulation of contaminants in their tissues and the consequent effects on biological processes (Dondero et al., 2005, Viarengo et al., 2007, Banni et al., 2011). The digestive gland of mussels has been used as a model system for studying the transcriptomic response to several environmental stressors and for the analysis of biomarkers and chemical loads in this organism (Banni et al., 2007, Dondero et al., 2011)

Among the effects of heavy metals in mussel highlighted, there is, for example, the activation of enzymes such as superoxide dismutase, catalase, glutathione peroxidase, metallothioneines and other cellular peroxidases. They constitute one of the first defense

mechanisms by oxidizing agents (Borković et al., 2005). However, these enzymes can be inhibited by metals, as demonstrated for cadmium and copper (Vergani et al., 2007).

Recently, many studies attempted to elucidate mechanisms in which heavy metals can stress organisms and the exact role of genes encoding proteins associated to the stress response such as heat shock proteins, oxidative stress, metallothioneins using proteomic and transcriptomic approaches (Dondero et al., 2005, Farcy et al., 2009, Lockwood et al., 2010, Negri et al., 2013). Overall, recent studies lead to the hypothesis that the load of reactive oxygen species (ROS) may be an important factor affecting the physiological costs of elevated environmental stress (Kamel et al., 2012, Negri et al., 2013)

In this study was observed and monitored the change in the functionality of some genes involved in the response to stress caused by the presence of metals.

According to various studies, metals are involved in the generation of free radicals (ROS) that are primarily responsible for the oxidative stress (Valko et al., 2005, Kim et al., 2009, Awasthi et al., 2013). The study of gene response of enzymes involved in ROS detoxification may provide insights about the effects of silver, first going to determine if there are differences between the effects produced by silver ion and that in the form of nanoparticles.

ROS formation and consequent damage are balanced by a range of cellular antioxidant defences including various antioxidant enzymes such as superoxide dismutase (SOD), catalase (CAT), glutathione peroxidase (GPX), glutathione-S-transferase (GST) as well as low molecular binding proteins such as metallothioneins (MT) that function as radical quenchers and as chain-breaking compounds (Livingstone, 2001, Dondero et al., 2005). In addition, the study was thorough going to observe the behavior of the genes responsible for the induction of Heat shock proteins (HSPs), molecular chaperones that assist in the modulation of stress response and protection against stress-associated cellular damages. Though originally identified as

proteins induced by heat stress, these proteins are up-regulated by a range of other stressors including oxidative stress, radiation, pH, salinity and xenobiotics (Lacoste et al., 2001, Fabbri et al., 2008, Thompson et al., 2012)

In particular, as regards the metallothioneins, were investigated the expression of the two major form studied: MT10 (10kDa) and MT20 (20kDa). MTs have the capacity to bind both physiological (such as zinc, copper, selenium) and xenobiotic (such as cadmium, mercury, silver, arsenic) heavy metals through the thiol group of its cysteine residues, which represents nearly the 30% of its amino acidic residues. Generally, in mussel, MT10 is the housekeeping isoform preferentially induced by essential metals, while the MT20 isoform has a very low constitutive expression, being specifically induced by toxic metals (Vergani et al., 2007).

As regard as HSPs, has been chosen to focus the study on the expression of three isoforms: HSP27(protect cells against oxidative stress by counteracting the accumulation of proteolysis-resistant large aggregates of oxidized proteins _lipofuscin_ which interfere with proteasome activity and are extremely deleterious to the cell), HSP70 (important mediators of intercellular signalling and transport) and HSP90 (important role in conformational protein regulation and cell signalling).

The expression level of these genes were monitored using quantitative reverse-transcription PCR (qRT-PCR), a routine technique for mRNA expression analysis, offering simplicity, high sensitivity, specificity, and high throughput (VanGuilder et al., 2008).

Real-time PCR has been successfully applied in the medical field, for example in the quantification of various DNA and RNA viruses in patients (Martell et al., 1999, Josefsson et al., 1999), in the detection of gene amplification (Bièche et al., 1998), mutations, or chromosomal rearrangements (Dölken et al., 1998), and in the quantification of gene expression (Bièche et al., 1999) or detection of various splice variants (Kafert et al., 1999).

Recently, real-time PCR was applied to studies of environmental samples in any environmental matrix (Makino et al., 2001, Guy et al., 2003, Okano et al., 2004, Dondero et al., 2005, Banni et al., 2007, Banni et al., 2011, Mo et al., 2012)

The advantage of the real-time PCR method over other PCR-based quantification methods is that it focuses on the logarithmic phase of product accumulation rather than on the end product abundance. This technique is therefore more accurate, since it is less affected by amplification efficiency or depletion of a reagent. In addition, real-time PCR measures template abundance over a large dynamic range of around six orders of magnitude (Heid et al., 1996). Finally, this method allows the simultaneous analysis of 96 samples in a short time and reduces the risk of contamination, as no post-PCR manipulation is required. The main disadvantage of real-time PCR is the need for a special thermocycler and reagents that are expensive compared to the equipment utilized by other PCR-based quantification methods.

To apply the technique of real time is first necessary to transcribe the mRNA into cDNA, as the amplification can only occur in the presence of DNA molecules. To do this is used method of reverse transcriptase-polymerase chain reaction (RT-PCR). The enzyme most commonly used is reverse transcriptase MMLV-RT and its derivatives engineered (Kotewicz et al., 1988), as it possesses limited RNase activity or even nothing in its recombinant form (H minus) (Gerard et al., 1997). The RT phase is triggered using specific primers of the target sequence, random hexamers or oligo-dT primers. The choice of primer depends on the desired specificity of transcription.

Although the concentrations of Mg^{2+} and deoxy-nucleotides (dNTP) require strict control, as the magnesium influence the enzymatic activity and a mixture of dNTPs unbalanced reduces the efficiency of the polymerase (Eckert and Kunkel, 1991).

In this technique, of great importance is the tail of about 200 residues of adenine (poly-A tail) that eukaryotic RNA present in their 3'-OH.

Transcription occurs in two steps: the first is that the primer, wherein the RNA is incubated with the enzyme reverse transcriptase, precursors triphosphate deoxyribonucleotides (dNTPs), buffer solution and divalent ions Mg^{2+} giving way, in the presence of the sequence complementary oligo(dT) or random hexamers, the formation of a cDNA strand. The pairing between two single strands of nucleic acid in general is defined annealing.

In the second step, the elongation, the primer provides a 3'-OH that uses reverse transcriptase to extend the chain by using as a template the transcript. This phase takes place at a temperature of about 50-60 ° C in 1 hour.

The real-time RT-PCR technique use fluorescent markers and combines the process of amplification and detection of a target RNA to allow monitoring of the PCR reaction in real time during the reaction.

The Real-Time PCR can be achieved through the use of intercalating dyes (eg, SYBR green) that bind in a nonspecific manner to all the DNA, or hybridization probes, specific for the fragment of interest, labeled with fluorescent molecules.

The second method employs the use of specific hybridization probes that can be of various types: Dual-labeled (like TaqMan probes), molecular beacons, scorpion and FRET probes (Fluorescence Resonance Energy Transfer).

The most widely used technology is represented by the TaqMan probes. Method was first reported in 1991 by researchers at Cetus Corporation (Holland et al., 1991), and the technology was subsequently developed by Roche Molecular Diagnostics for diagnostic assays and by Applied Biosystems for research applications

The TaqMan assay using the nuclease activity in 5'of the DNA polymerase to hydrolyze a hybridization probe bound to its target amplicon (Gut et al., 1999).

The TaqMan probe is an oligonucleotide which, as the PCR primers, is designed to be complementary to the target sequence to be amplified. It containing a fluorescent Reporter dye (R, fluorophore which emits high-energy fluorescence) at the 5' end and Quencher (Q, fluorophore at low energy that turns off the fluorescence of the reporter) at the 3' end.

If there is no amplified probe complementary to the amplicon during PCR, the probe remains free. Because the exonuclease activity in 5'of the Taq polymerase is specific for the double helix (Heid et al., 1996) probes not bound remain intact and is not detected fluorescence. Conversely, if the amplicon is correctly detected the probe can hybridize with this amplicon after the step of denaturation. In this type of configuration, the Quencher molecule prevents the emission of fluorescence from the Reporter.

During each PCR cycle, in the phase of extension of the DNA strand, the enzyme continues to move from the free end towards the bifurcation of the duplex, where the division is originated (Lyamichev et al., 1993). When the enzyme Taq polymerase encounters the 5'end of the probe makes the detachment of the Reporter thanks to the intrinsic 5'-3' exonuclease activity, keeping the probe in a fork structure. In this way the fluorophore goes into solution, no longer sustained inhibition of Quencher and emits fluorescence (Fig. 24).

When the PCR cycles proceeds, resulting in more amplification of the target molecules proportionally fluorescent signal will also increase.

The highest fluorescent signal is obtained when the two dyes are at the ends 3'and 5' of the probe, probably due to a more efficient division by the polymerase.

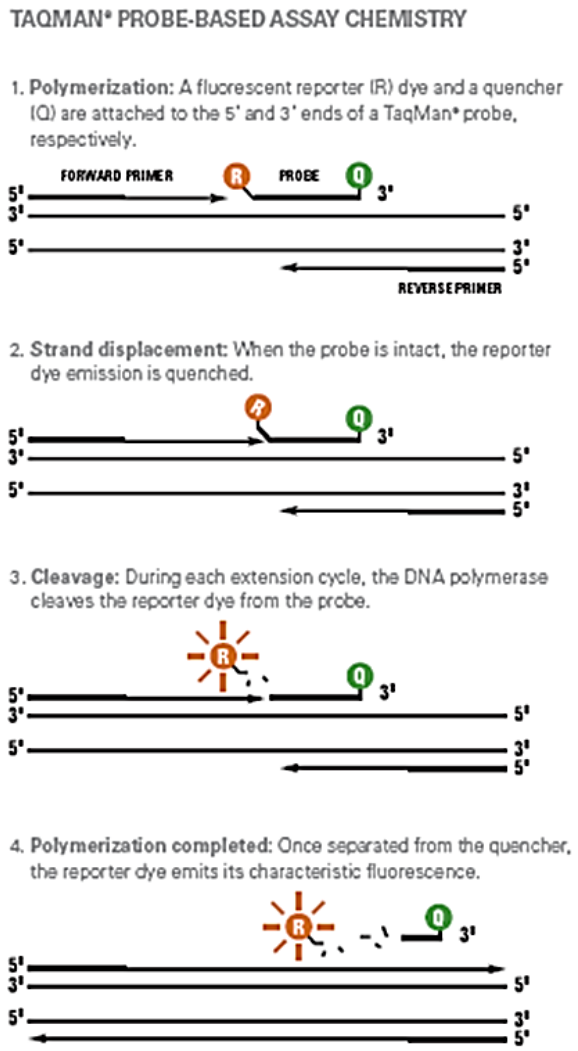

Fig 24- Chemistry of TaqMan probes

The advantages of TaqMan Assay are that specific hybridization between probe and target is required to generate fluorescent signal, probes can be labeled with different, distinguishable reporter dyes, which allows amplification and detection of two distinct sequences in one reaction tube and post-PCR processing is eliminated, which reduces assay labor and material costs

The main disadvantage of TaqMan assay is that synthesis of different probes is required for different sequences sometimes makes it difficult.

As already said, the qRT-PCR measuring the amplification in real time during the exponential phase of PCR, that is when the amplification efficiency is affected minimally by the variables

of the reaction. This allows to obtain more accurate results than the traditional PCR "end point". In a typical reaction, the PCR product is doubled with each cycle of amplification. Since it takes several cycles to ensure that enough product is detectable, the plot of the fluorescence on the number of cycles exhibits a sigmoid. In the final cycle, the reaction substrates become scarce, the PCR products do not double and the curve begins to flatten. The point on the curve where the amount of fluorescence begins to increase rapidly, usually some deviations above the baseline, is called the threshold cycle (Ct value). The diagram of Ct on template DNA is linear, so a comparison of the Ct values between multiple reactions allows to calculate the concentration of the nucleic acid that you want to quantify. The slope of this line also provides a measure of the efficiency of PCR. For each sample, an amplification curve is obtained whose Ct (= Threshold Cycle) is inversely proportional to the initial amount of template.

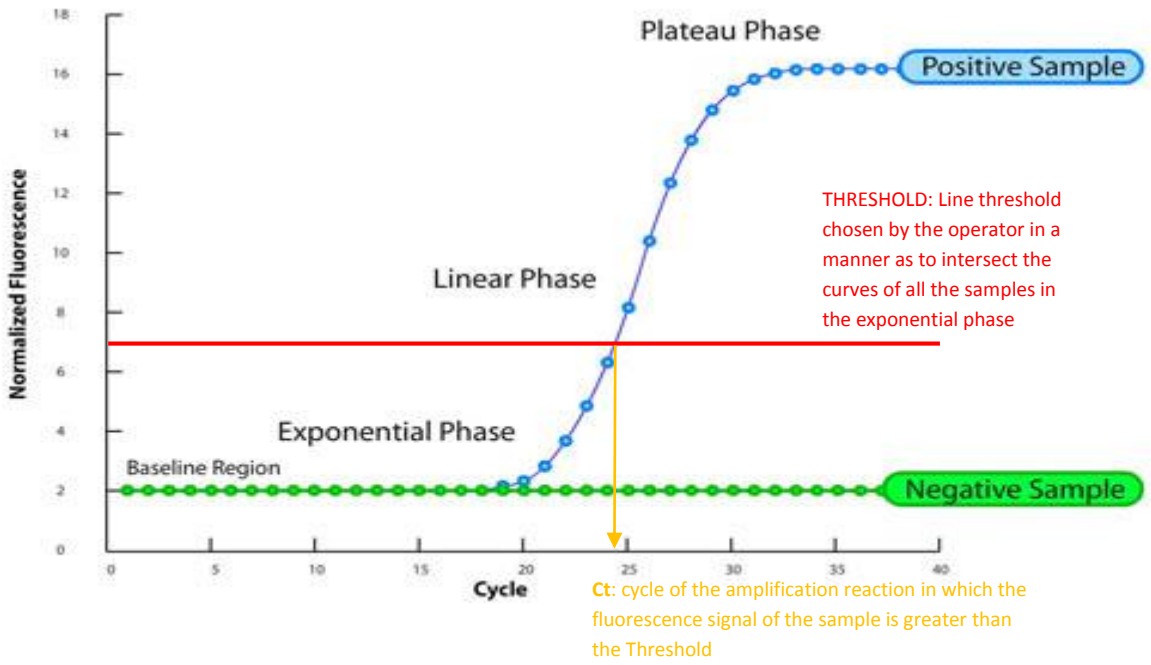

To calculate the normalised relative gene expression levels (fold induction), real time quantitative PCR data were analysed using the relative expression software tool (REST), where the mathematical model is based on mean threshold cycle differences between the sample

and the control group (Pfaffl et al., 2002). A non-parametric statistical test was also obtained using REST

The analysis quantitative relative of data obtained is performed by comparing the Ct values to determine the change of expression of a target gene. To do this is compared this value of Ct with that of another sample chosen as the endogenous control gene (gene constitutively expressed in all the analyzed samples necessary to normalize the data with respect to the amount of DNA loaded and variations in the efficiency of the reaction) and a calibrator (for example, t0 of the experiment)

The following calculationwas applied:

- the target is normalized to an endogenous control (r) constitutively expressed (ΔCt)

  $Ct_{target\ gene} - Ct_r = \Delta Ct$

- Each ΔCt thus obtained is compared with the ΔCt of the calibrator (cb)

  $\Delta ct_{target} - \Delta Ct_{cb} = \Delta\Delta Ct$

- is then applied the formula: $2^{-(\Delta Ct_r - \Delta Ct_{cb})} = 2^{-(\Delta\Delta Ct)}$

The value thus obtained allows to determine the relative concentration of the target

In this part of the work a molecular investigation has been applied to samples taken from mussels *Mytilus galloprovincialis* treated in different ways:

- First step: analysis of samples treated for 4 days at different silver forms at high concentrations. Gene expression of the main genes involved in oxidative stress and metallothioneins has been investigated in organisms treated with AgNP 8nm, 50nm AgNP and $AgNO_3$ (for exposure see chapter 2). Samples were exposed at different concentrations of silver (10 mg/L, 1 mg/L , 0.1 mg/L and 0.01 mg/L). Analysis wasn't carried out for $AgNO_3$ 0.01 mg/L.

- Second step: was observed the temporal evolution in gene expression for target genes during long-term exposure (28 days) of organisms treated with AgNP 8nm at 0.2 µg/L, 2 µg/L and 20 µg/L (for exposure see chapter 3).

MATERIALS AND METHODS

Animals and treatments

Short terms exposures and long term exposure have been already described in Chapter 2 and Chapter 3 respectively.

RNA extraction

Total RNAs were extracted from glands and gills of individuals. For each treatment 8 organisms were used for obtain eight biological replicates and three technical replicates.

The total RNA purification kit, 5-PRIME PerfectPure RNA Tissue Kit (5 PRIME Inc, Gaithersburg, MD) was used for RNA purification and the protocol of the manufacturer's instructions was followed. The extracted RNA quantification was performed using spectrophotometric technique and quality of each RNA preparation was confirmed by TBE agarose gel electrophoresis in the presence of formamide (Sambrook et al., 1989).

Reverse transcriptase-polymerase chain reaction (RT-PCR)

In the experiment, 0.5 µg of RNA were reverse transcribed using 200U of M-MuLV H minus Reverse Transcriptase (Fermentas, Thermo Fisher Scientific Inc.), 250 ng/µl of Random Hexamer Primer (Fermentas, Thermo Fisher Scientific Inc.), 0.5 mM dNTPs and 1x reaction buffer (Tris-HCl, KCl, $MgCl_2$, DTT) (Fermentas, Thermo Fisher Scientific Inc.) in a final volume of 20µl.

The thermal profile was designed as described by the manufacturer, except an extra 20 min step at 55°C, which was added to the standard 60 min extension at 42°C (preceded by a random hexamers annealing step of 10 minutes at 25 C). Lastly, the enzyme was deactivated with a step of 10 min at 70°C.

The result of the reaction was brought to 200 µl final volume with DEPC-water.

Determination of silver concentration in mussel tissues

Gills and digestive glands were dissected from soft tissues of mussels, serially washed in clean seawater, passed extensively under cold tap water, damped and frozed to -20° until analysis. One (1) g of tissue from single individuals were thawed and homogenized with the addition of 5 ml deionized water. Samples were digested acid in a microwave oven with 50 ml of a 3:1 mixture of concentrated HCl:HNO_3 (aqua regia) and further analysed by ICP-MS analysis according to the referenced procedure EPA 3051A. LOD was 0.5 µg/L in the acid matrix. The analysese were carried out by an external laboratory.

Determination of soluble silver concentration in water

50 ml water samples were withdrawn from each tank at regular intervals of 0, 1, 4, 24 h from water/chemical renewal. 10 ml aliquots were immediately subjected to ultracentrifugation at 100,000 g for 2 h at 4°C to collect the dissolved (ionic) silver fraction. The supernatant was diluted 1:5 with concentrated HCl:HNO_3 3:1 (aqua regia), then silver content analysis was performed by Inductively-Coupled Plasma Mass-Spectrometry (ICP-MS). The sensitivity limit (LOD) for silver was 0.5 µg/L in the acid matrix. Samples were delivered for analysis to an external laboratory, which analyzed the samples according to a standard referenced procedures (UNI EN ISO 17294-2:2005).

Real Time quantitative Reverse Transcription PCR (Real-time qRT-PCR)

2 µl of cDNA obtained by RT-PCR were used for the amplification of several target genes. The reaction mixture in which they were added contained 1X iQ™ Multiplex Powermix (BioRad Laboratories Srl, Milan, Italy), 0.3 µM of each primer (sense and antisense) and 0.1 µM of each probe (see Table below). Final volume of reaction was 7 µl.

Each plate (386 wells) was loaded as a triplex according to the marking of the probes and negative controls with no template DNA were run in each plate.

cDNA was amplified in a CFX384 Real-Time PCR detection system (BioRad Laboratories Srl, Milan, Italy). The thermal protocol used was as follows: 3 minutes at 95 ° C for the activation of the enzyme, followed by 40 cycles (10 seconds at 95°C, 60 seconds at 60°C)

Relative expression data were geometrically normalized to 18S rRNA, an invariant actin isotype, the ribosomal protein riboL27 and glyceraldehyde 3-phosphate dehydrogenase.

qRT-PCR was performed with eight biological replicates and three technical replicates. Statistical analyses were carried out on the group mean values using a random reallocation test (Pfaffl et al., 2002).

Housekeeping genes	Reporter dye	Probe	Sense primer	Antisense primer
G3PDH (AJ625142)	CY5	CTGCTCCTGTTGTCT CCACGGAAGTCTT	TCTGAGGGTCCAAT GAAGGGTG	GAGCGATGCCAGCT TTGGC
18S (L33452)	sulforhodamine 101 acid chloride (TEX)	ACCACATCCAAGGA AGGCAGCAGGC	CGGAGAGGAGCAT GAGAAAC	CGTGCCAGGAGTG GGTAATTT
ACT (AF157491)	6-carboxyhexa fluorescein (HEX)	ACGCCAACACCGTC TTGTCTGGTGG	GTGTGATGTCGATA TCCGTAAGGA	GCTTGGAGCAAGT GCTGTGA
RiboL27 (AJ625928)	5-Carboxynaptho fluorescein (FAM)	TGCGCCATTCAGCA CAAGAACTACCT	AAGCCATGGGCAA ATTTATGAAAA	TTTACAATGACTGC TTTACGACCT
Target genes		**Probe**	**Sense primer**	**Antisense primer**
GST (AF527010)	FAM	TCCATGTTACACAG ATGATGACGGTTTC	CTGGAAACCAAAGA TGCAATTTG	TCTGCCAAGATATG CCAGTATT
SOD (FM177867)	HEX	TCCTGTCACTGTCA CTGCTGAATCACCA	AGGAACAGTCGCTT TCAGTCAAC	TCCTGGAGCTAGCC CAGTTAAC
CAT (AY580271)	TEX	CCAGGTGTCCTTCC TGTTCTCTGACCG	ATTACACTTCGACC AGAGACAACC	GTCCATCCTTGTTG ACCGTCTTAA
HSP27 (AJ625244)	HEX	CTTGGTGTCCAGTG ACAGCCACAGCA	TTGTCCCACAGAAG GTCGGG	ACAGACCGTGGAA CTGTCATCT
HSP70 (AJ624615)	TEX	AGCAGCCTTGTCTA GTTTGGCATCGC	CCACCTACCAAGAC AATTTCATGG	ACAAGCAAGTGTTG AGATTGACTC
HSP90 (AJ625621)	FAM	AAGTCCTCGCTTCC TCAGTCTCTCAACA	CACAGGTGAATCCA AAGATGTTGT	ACTCATCAATGGGG TCTATCATGT
GPX	CY5	AGCTGCCACCAAGG ACCGTCTTGTT	TTGTTTTCTGTAGG CCGTGTGA	CTACTACCGCTAGA CAGCCTAGA
MT10	SybrGREEN	GTGCTCGGGCGCC GACTG	TGTAGCGGTGAAG GTTGTCG	CGCACAGCTACCTG AACACT
MT20	SybrGREEN	TCCGCGCCCTTCCA T	GGCTGGACCTTGTA ACT	GGTACCTGAACATC TGCAA

Protein extraction and 2-DE gel electrophoresis

The tissue -digestive glands and gills- of five mussels (single animal) for treatment were homogenized in a lysis buffer according to the method described in Dondero et al. (2010). Protein precipitation was performed in 20% v/v cold trichloroacetic acid and the pellet was resuspended in a typical solubilization buffer (7M Urea, 2M Thiourea, 4% CHAPS, 20 mM DTT, 0.5% Triton X-100, 0.5% Biorad ampholite solution). The protein concentration was assayed using the Bradford reagent (SERVA).

For the first dimension (IEF), immobilized strip gels pH 4-7 linear, 7 cm (BioRad Laboratories Srl, Milan, Italy) were used to separate 100 µg of proteins. IEF was carried out as describe by Boatti et al. (2012) on an IPGphor unit (GE Healthcare Europe GmbH).

For the second dimension, the strips were first equilibrated and proteins reduced in an SDS equilibration buffer (50 mM Tris-HCl pH 8.8, 6 M Urea, 30% v/v glycerol, 2% w/v SDS) containing 10 mg/mL DTT for 15 min, rinsed with distilled water and then alkylated with 25 mg/mL of iodoacetamide for 10 min (Marsano et al. 2009)

SDS-PAGE on 12% gels was performed at 15 mA/gel for 15 min and 30 mA/gel for 1.5 h at 10°C with a Mini-Protean cell (BioRad Laboratories Srl, Milan, Italy). To check the quality of protein extraction, the polyacrylamide gels (one gel for treatment) were fixed in a solution containing 40% methanol and 10% acetic acid and stained with Colloidal Coomassie brilliant blue G250 (BioRad Laboratories Srl, Milan, Italy).

2-DE Western blotting and carbonyls detection

The proteins obtained from digestive glands and gills after the 2-DE separation were electroblotted on PVDF membrane (BioRad Laboratories Srl, Milan, Italy) for antibody-mediated detection.

Carbonyls were chemical labeled by 2,4-Dinitrophenylhydrazine (DNPH), then antibody-mediated detected for Dinitrophenylhydrazone (DNP) and visualized by HRP-conjugate secondary antibody, using Protein Carbonyl Immunoblot kit (Cell Biolabs, San Diego, CA, USA), with adaptation for 2-D electrophoresis. Images were acquired using a ChemiDoc XRS (BioRad Laboratories Srl, Milan, Italy) and analyzed using PDQuest Software version 7.3.1 (BioRad Laboratories Srl, Milan, Italy) (Marsano et al., 2009).

Gene expression study: short term effects

We investigated gene expression patterns in the digestive gland and gills of mussels exposed to different silver forms (5 nm, 50 nm ENPs as well as silver nitrate) for four days (short exposures) at different concentration levels (see also Chapter 2 for details on exposures and

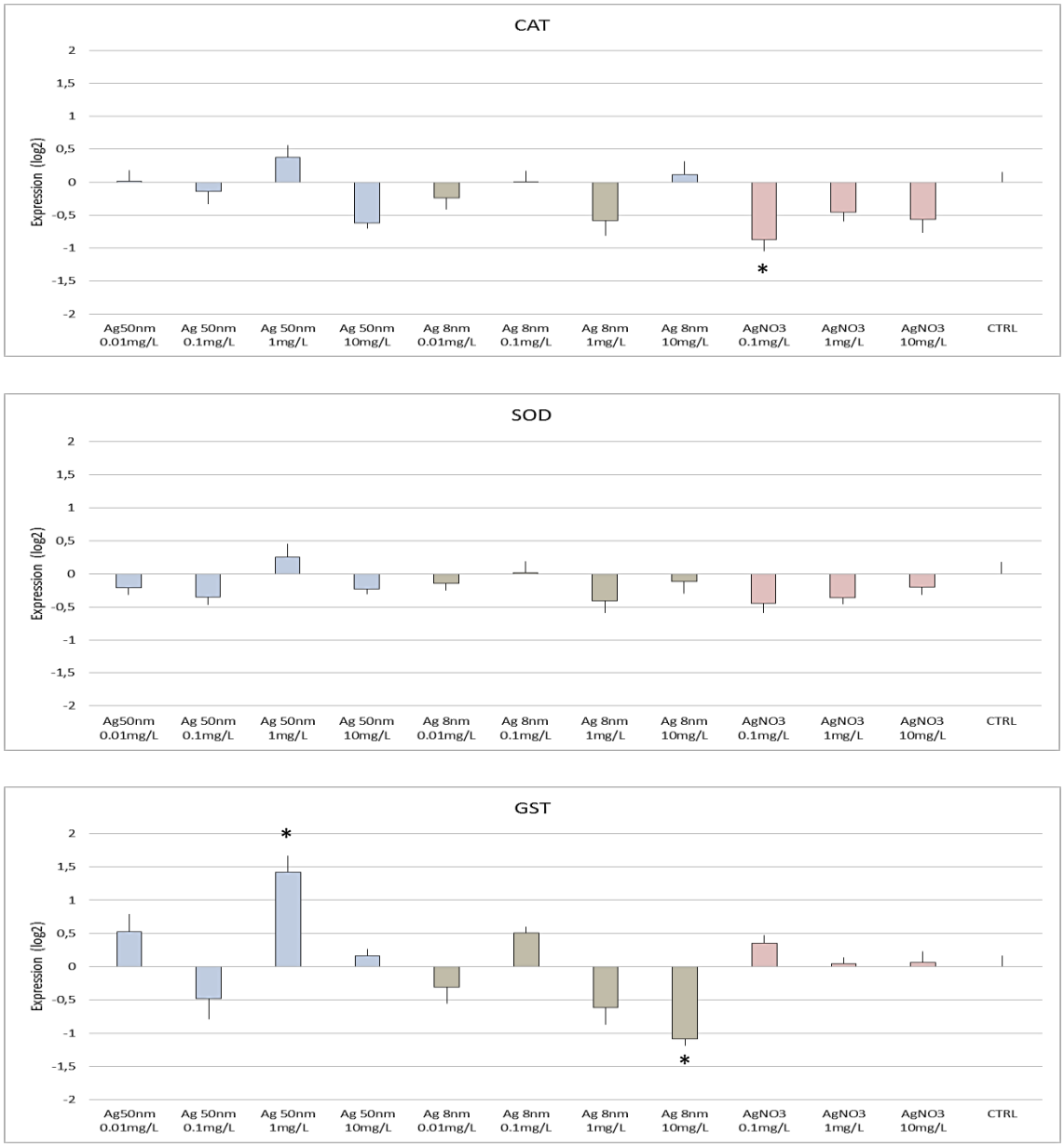

***Fig 25** - Relative mRNA levels of oxidative stress genes (CAT, SOD, GST) in digestive gland of mytilus exposed for 4 days to different form and concentrations of silver. All data -group mean ± SEM- were normalized with respect to control (CTRL) using the geometric mean expression levels of actin, ribonucleoprotein L27 and 3GPDH.* different from control p < 0.05 according to a non parametric mean group randomization test, n=8 (Pfaffl et al., 2002)*

organismic responses). To this aim, a battery of oxidative stress responsive genes made of catalase (CAT), superoxide dismutase (SOD), a soluble glutathione transferase (GST) were considered. Furthermore, the mRNA levels of two heavy metal homeostasis sequences (metallothionein MT10 and MT20) (Dondero et al., 2005) were analysed. Fig. 25 depicts relative mRNA levels of CAT, SOD and GST found in the digestive gland of Ag treated specimens with respect to control not exposed ones. CAT levels showed a trend of down-regulation for the effects of ionic Ag, but no effects for ENPs. SOD levels displayed only random fluctuations. GST levels showed some significant modulations for the treatment to 1 mg/L 50 nm ENPs (~3 fold overexpression) and 10 mg/L 5 nm ENP (~2 fold downregulation).

In the digestive gland metallothionein genes showed quite unexpected patterns (Fig. 26).

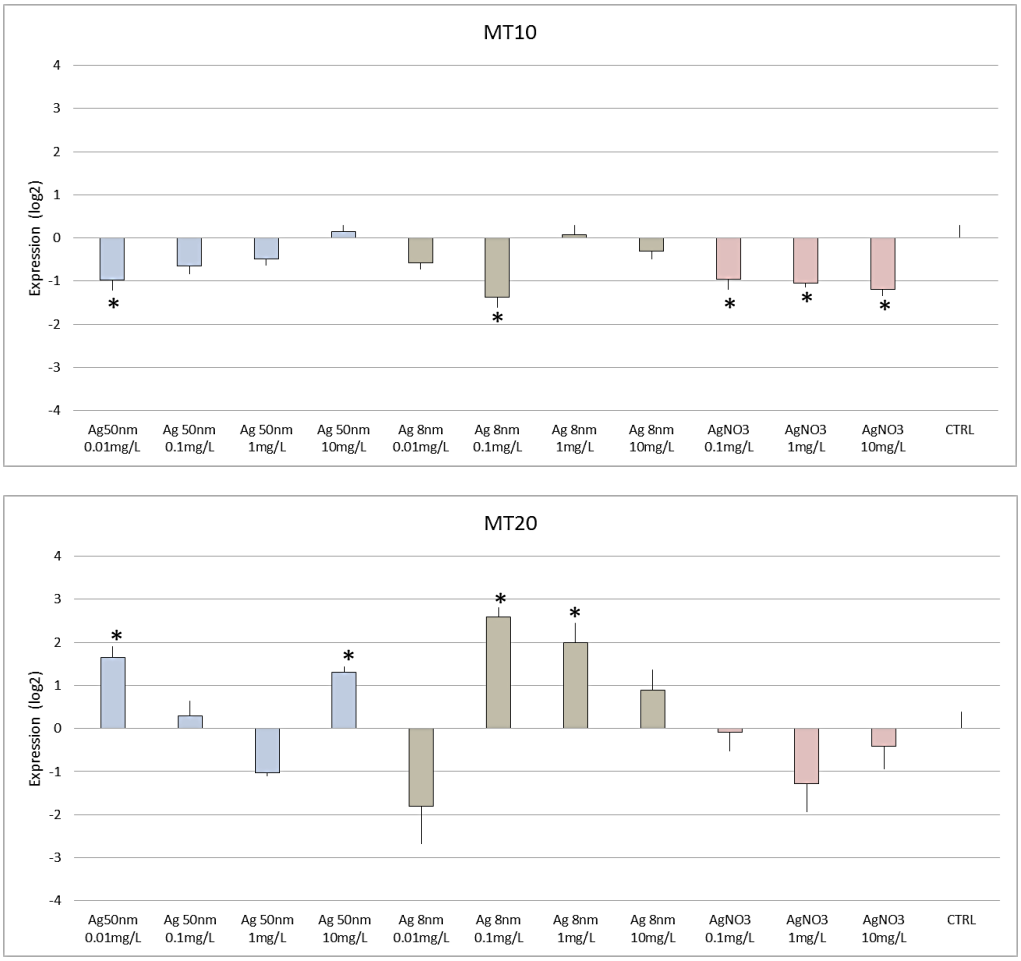

***Fig 26** - Relative mRNA levels of metallothioneins genes (MT10, MT20) in digestive gland of mytilus exposed for 4 days to different form and concentrations of silver. All data -group mean ± SEM- were normalized with respect to control (CTRL) using the geometric mean expression levels of actin, ribonucleoprotein L27 and 3GPDH.* different from control p < 0.05 according to a non parametric mean group randomization test, n=8 (Pfaffl et al., 2002)*

In particular, mRNA levels of the MT10 isogene, that is constitutively expressed but yet inducible (Dondero et al., 2005), were often down-regulated. This outcome was more consistently found for the effects of silver nitrate. However, it should be reminded that 1 mg/L and 10 mg/L Ag^{+} were lethal concentrations (Chapter 2, Figure 1), therefore these effects could be representative of an adverse outcome pathway due to a pathological condition., rather than an adaptive response. The cognate MT20 gene, that is involved in xenobiotic metal response (Dondero et al., 2005), conversely, displayed over-expression for the effects of either ENPs but not nitrate.

In gills (Fig. 27), the colloidal silver forms elicited fair up-regulated levels for CAT, however, these were not often statistically significant due to a high degree of inter-individual variability. SOD showed a similar patter, but at lesser intensity. Nitrate produced only modest effects on latter gene, but a significant down-regulation on GST at 0.1 mg/L that was the NoEC for mortality (Chapter 2, Fig. 1). In gills, however, MT genes functioned with a clearer heavy metal response than in digestive gland (Fig. 28). MT10 mRNA levels, in fact, increased significantly in almost all tested conditions, nitrate having shown the highest effects (by 7 fold). The 5 nm ENPs response did not appear very consistent, but the full confirmation of the MT system activation came from MT20 expression patterns. In this case, all silver forms were effective at all tested concentrations, the higher fold change being recorded for the 5 nm ENPs at 10 mg/L (~80 fold) and nitrate at 0.1 mg/L (64 fold).

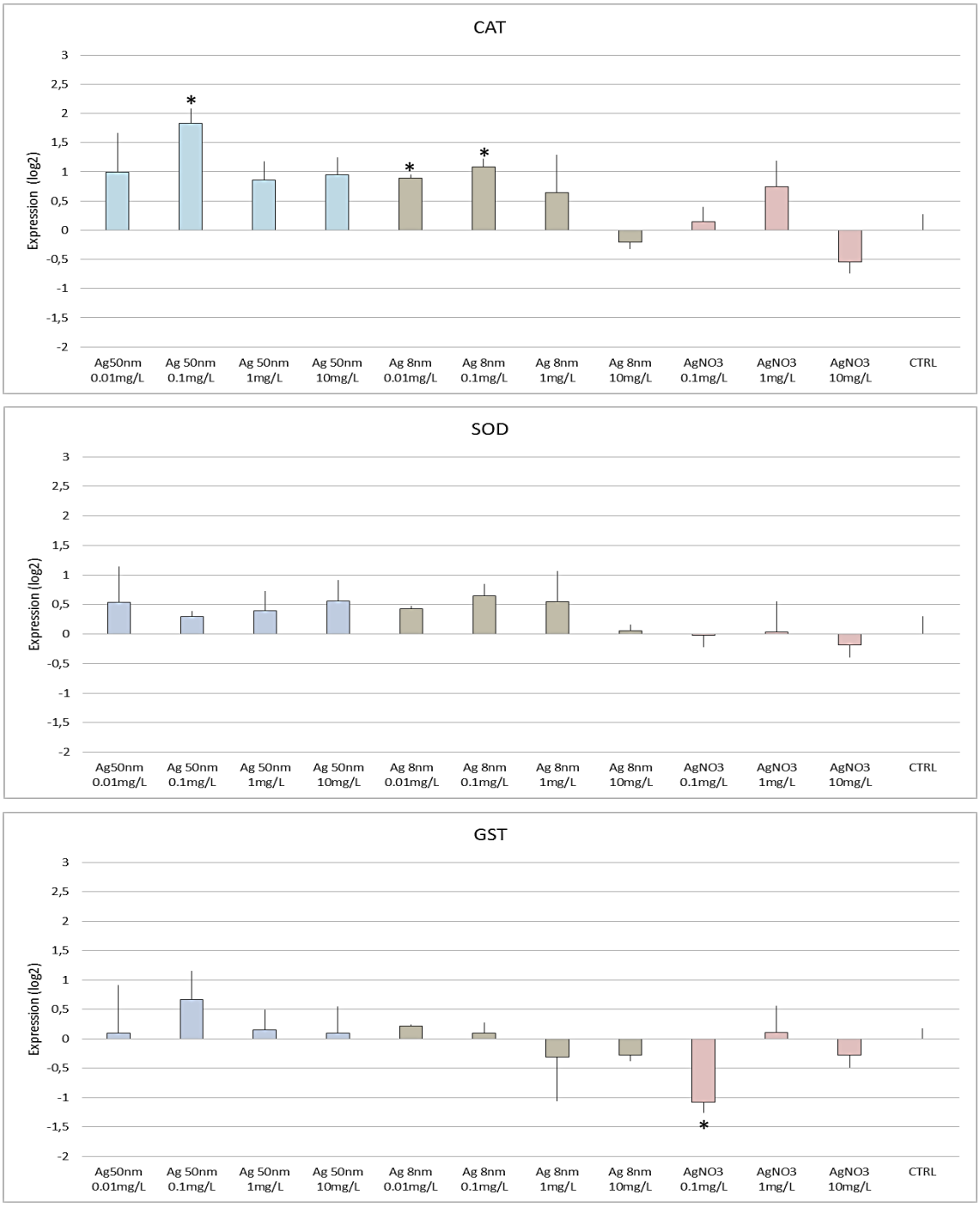

Fig 27- Relative mRNA levels of oxidative stress genes (CAT, SOD, GST) in gills of mytilus exposed for 4 days to different form and concentrations of silver. All data -group mean ± SEM- were normalized with respect to control (CTRL) using the geometric mean expression levels of actin, ribonucleoprotein L27 and 3GPDH.* different from control p < 0.05 according to a non parametric mean group randomization test, n=8 (Pfaffl et al., 2002)

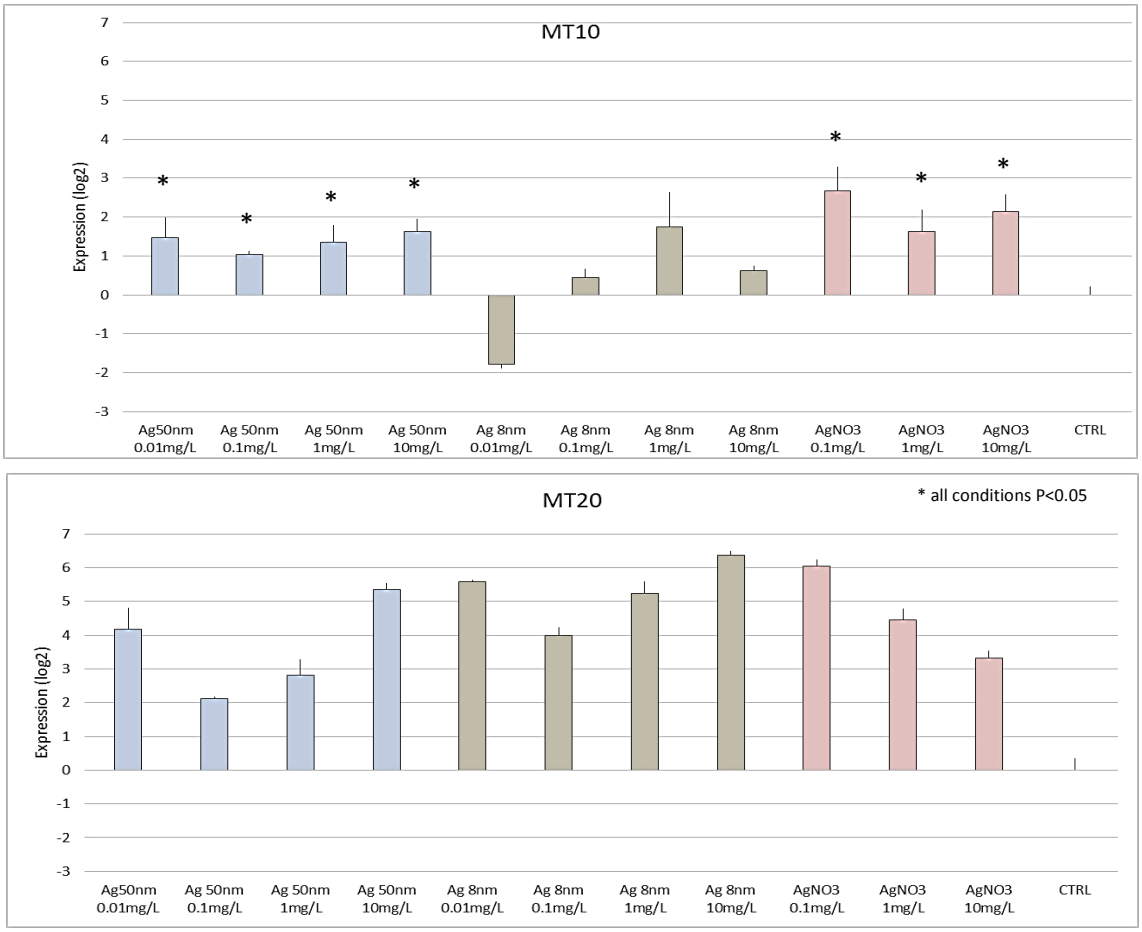

Fig 28- Relative mRNA levels of metallothioneins genes (MT10, MT20) in gills of mytilus exposed for 4 days to different form and concentrations of silver. All data -group mean ± SEM- were normalized with respect to control (CTRL) using the geometric mean expression levels of actin, ribonucleoprotein L27 and 3GPDH.* different from control p < 0.05 according to a non parametric mean group randomization test, n=8 (Pfaffl et al., 2002)

From aforesaid results, yet in particular from the differential metallothionein response observed in the two mussel tissues (Figures 26 and 28), it appeared that gills represented a common target organ for all silver source while the digestive gland was much more impacted from Ag ENPs than the ionic form. To confirm this hypothesis, mussels were exposed to 0.1 mg/L either ENPs (5 nm and 50 nm) or silver nitrate for 4 days and Ag content was further determined in digestive gland and gills. As expected, this analysis pointed out distinct bioaccumulation patterns depending on the initial silver source (Fig. 29). When colloidal forms were provided 65% and 61% of the metal was found in the digestive gland respectively for 5 nm and 50 nm ENPs. By contrast only 6% of silver was found in such tissue when $AgNO_3$ was provided, the most being found in gills. It is worth noting that the average soluble silver

fraction measured in the water column for 5 nm and 50 nm ENP during the exposure was 40% and 49%, respectively (data not shown), thus reflecting and yet mechanistically explaining the bioaccumulation patterns.

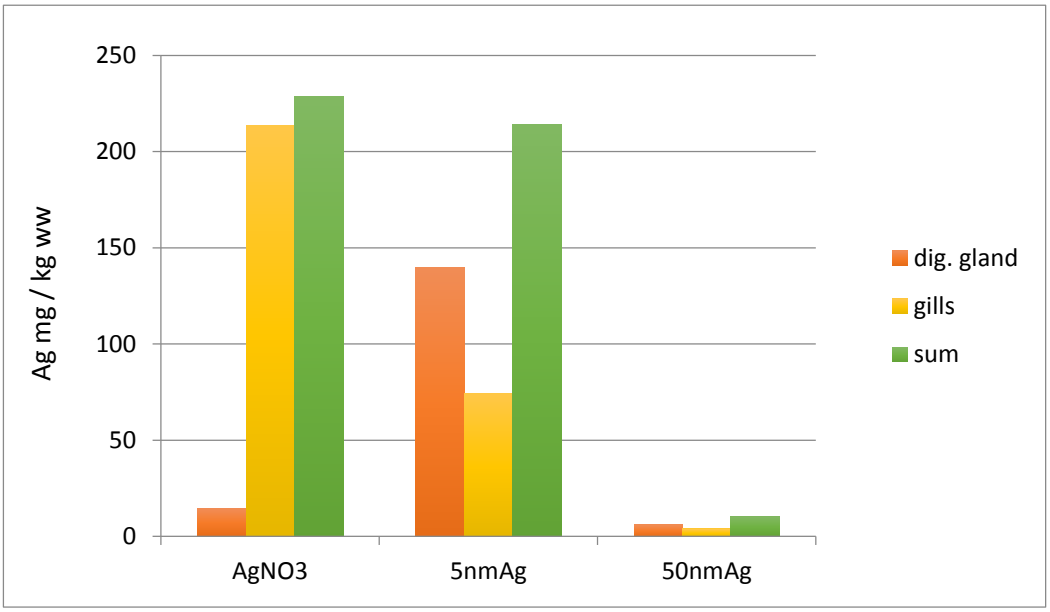

Fig 29- Ag accumulation in digestive gland and gills. Shown are median values from 8 specimens exposed to 0.1 mg/L silver in the initial form of $AgNO_3$, 5 nm Ag ENP and 50 nm Ag ENP

Molecular adaptive response to Ag ENP.

Transcriptomics dynamics in the two target organs (i.e. digestive gland and gills) were studied in long-term exposures (4 weeks). To this aim mussels were treated in microcosms to 5 nm AgENPs at low concentrations, 0.2; 2.0 and 20.0 µg /L /d (nominal concentrations) and sampled at regular intervals of 1 d, 7 d, 14 d and 28 d (more details of the exposure are presented in Chapter 3). Only 5 nm ENPs were employed in this experiment since these particles displayed much longer half-life in seawater than 50 nm ENPs (see Chapter 2 for details). Real time quantitative PCR with Taqman probe chemistry was used to study mRNA level dynamics of a larger gene battery including also glutathione peroxidase (GPX) and heat shock proteins HSP70, HSP90 and HSP27.

In digestive gland, -the specific target organ of ENPs- MT10 reached a new higher steady state, in particular at the highest exposure level (20 µg/L, at which differences were statistically significant). MT20 showed wider fluctuations across time than MT10 but at 20 µg/L there was was a robust and significant increment of its mRNA (on average of about 8 fold) (Fig. 30).

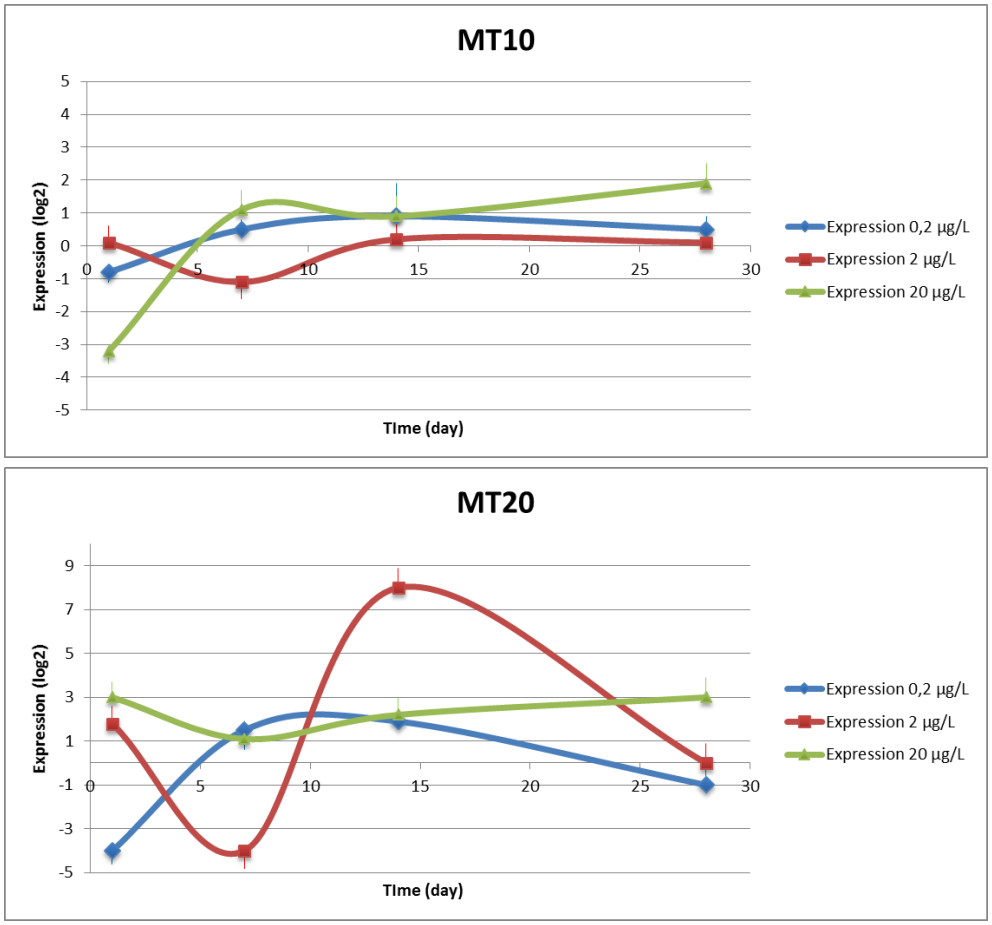

***Fig 30** -Time series analysis of metallothionein (MT10, MT20) relative mRNA levels in the digestive glands of mussels exposed to 5 nm AgENP for 28 days. Shown is the average value ± SEM (n=6) of [Ag]exp$_t$/CTRLexp$_t$ at each time (t) and for each AgENP exposure level ([Ag]).*

Also CAT, SOD, GST and GPX showed temporal trends with common features (Fig. 31). An important remark is that samples treated with the highest ENPs concentration (20 µg/L) showed always elevated mRNA relative abundances at the end of the exposure period. This result would indicate the possible occurrence of an anti-oxidant response.

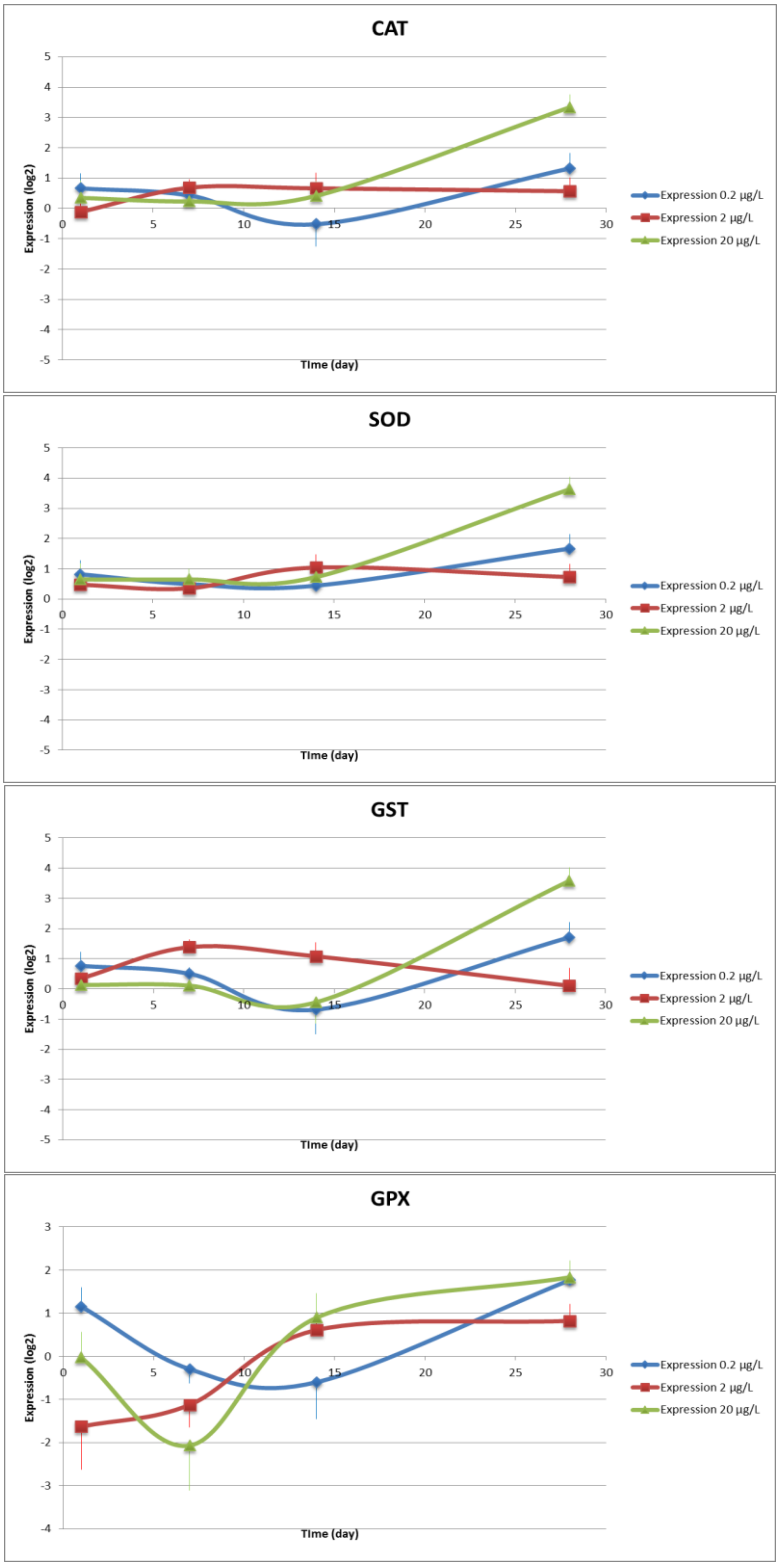

***Fig 31** -Time series analysis of oxidative stress related genes (relative mRNA levels) in the digestive glands of mussels exposed to 5 nm AgENP for 28 days. Shown is the average value ± SEM (n=6) of [Ag]exp$_t$/CTRLexp$_t$ at each time (t) and for each AgENP exposure level ([Ag]).*

The HSP probe set showed a few significant fluctuations across time as the case of HSP27 (Fig. 32). However, at the end of the exposure period their mRNA levels appeared to be compensated, except HSP70 showing significant up-regulation at 20 µg/L.

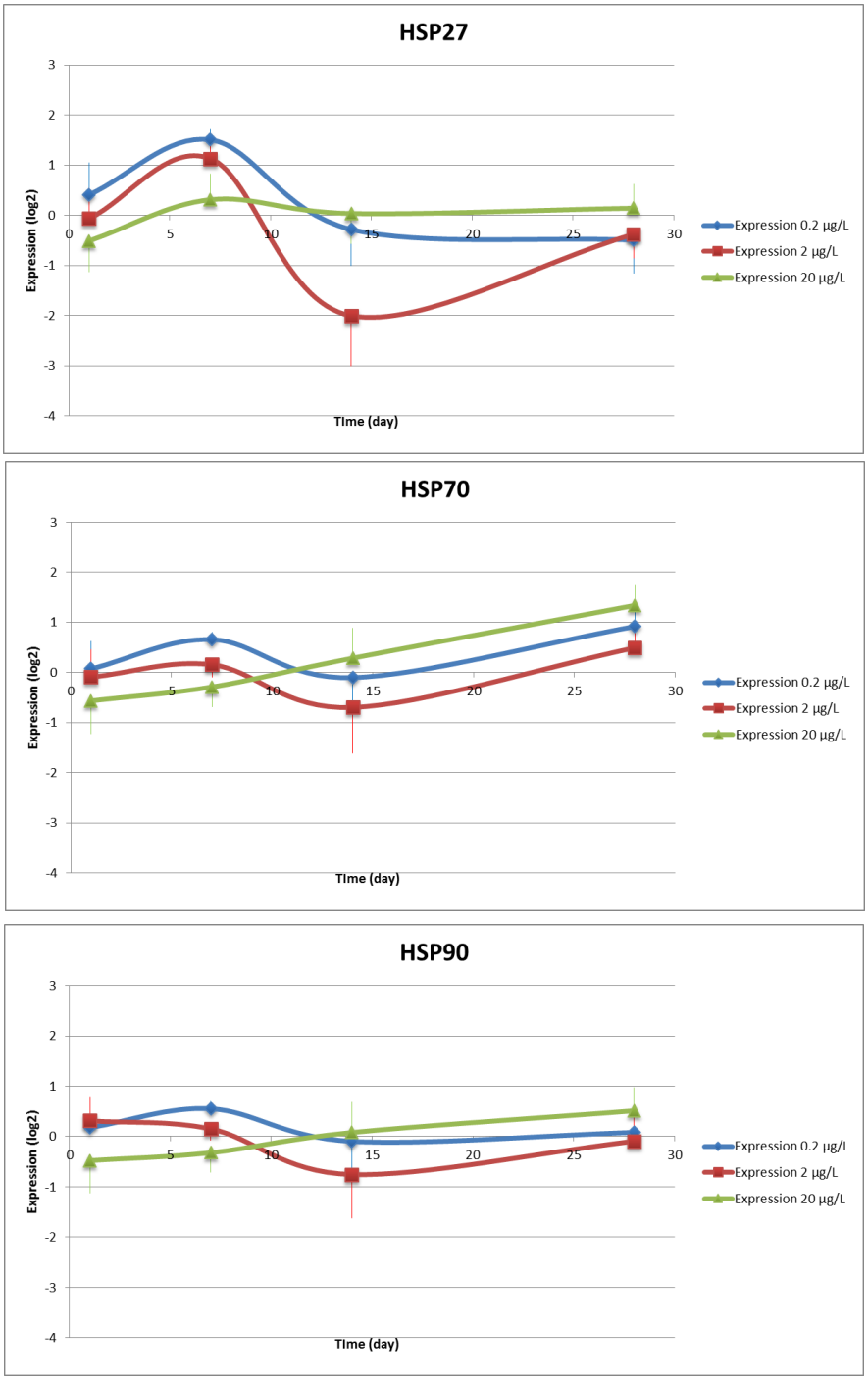

***Fig 32** - Time series analysis of HSPs (relative mRNA levels) in the digestive glands of mussels exposed to 5 nm AgENP for 28 days. Shown is the average value ± SEM (n=6) of Ag]exp$_t$/CTRLexp$_t$ at each time (t) and for each AgENP exposure level ([Ag]).*

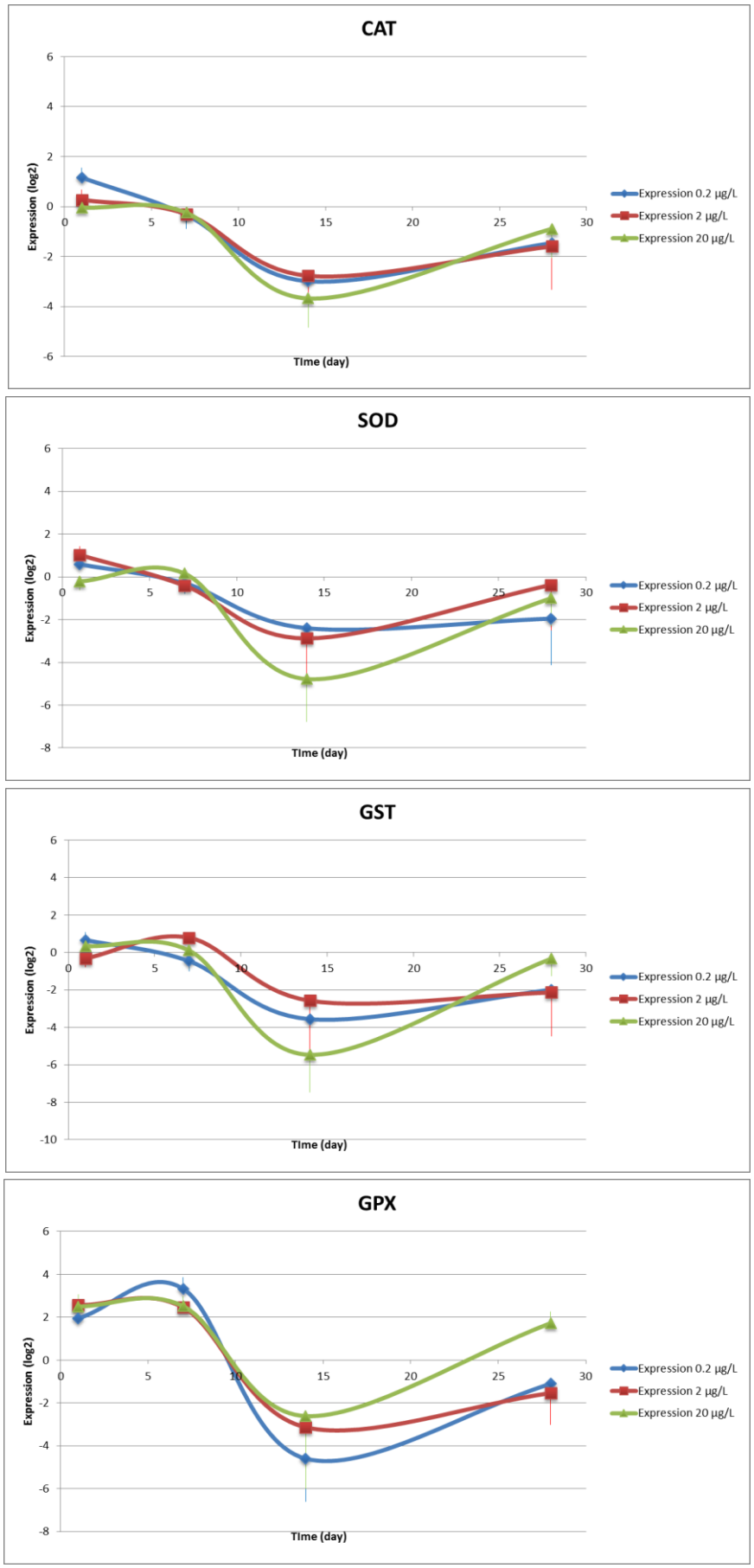

***Fig 33** - Time series analysis of oxidative stress related genes (relative mRNA levels) in gills of mussels exposed to 5 nm AgENP for 28 days. Shown is the average value ± SEM (n=6) of Ag]exp$_t$/CTRLexp$_t$ at each time (t) and for each AgENP exposure level ([Ag]).*

In gills, the dynamics found for oxidative stress related genes appeared to be compliant with an adaptive response (Fig. 33). All patterns, in fact, were characterized by a huge down-regulation in the middle of the exposure period and a further recovery. Among this group, GPX was the only gene showing a significant up-regulation at the end of the exposure period and this effect, found at 20 µg/L, was concentration dependent. In same condition, also metallothionein relative mRNA abundances were higher, indicating a fair Ag accumulation at the end of the exposure period (Fig. 34).

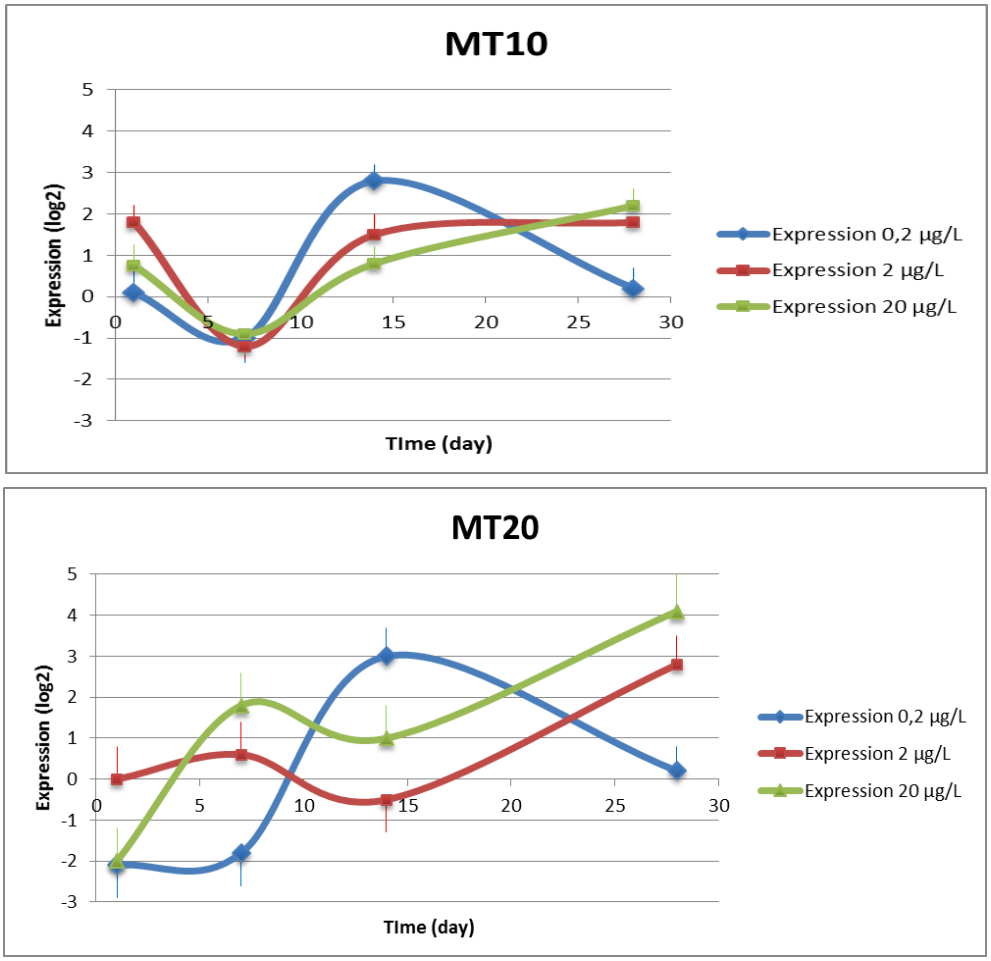

***Fig 34** - Time series analysis of MT (relative mRNA levels) in gills of mussels exposed to 5 nm AgENP for 28 days. Shown is the average value ± SEM (n=6) of Ag]exp$_t$/CTRLexp$_t$ at each time (t) and for each AgENP exposure level ([Ag]).*

In gills, HSP displayed more severe patterns than those found in the digestive gland. HSP27 expression showed an early increase at day 1, then compensation to normal pre-exposure levels occurred for the two lower ENPs concentrations, but not for the highest level (Fig. 35).

The other two genes, HSP70 and HSP90 were significantly and dose dependently up-regulated at the end of the exposure period. Activation of HSP genes reflects the occurring of a stress syndrome (Fabbri et al., 2010); Furthermore, this represents a proxy of serveral stress related processes, such as protein refolding, increased proteolysis (ubiquitin related), endoplasmic reticulum trafficking, exocytosis, etc.

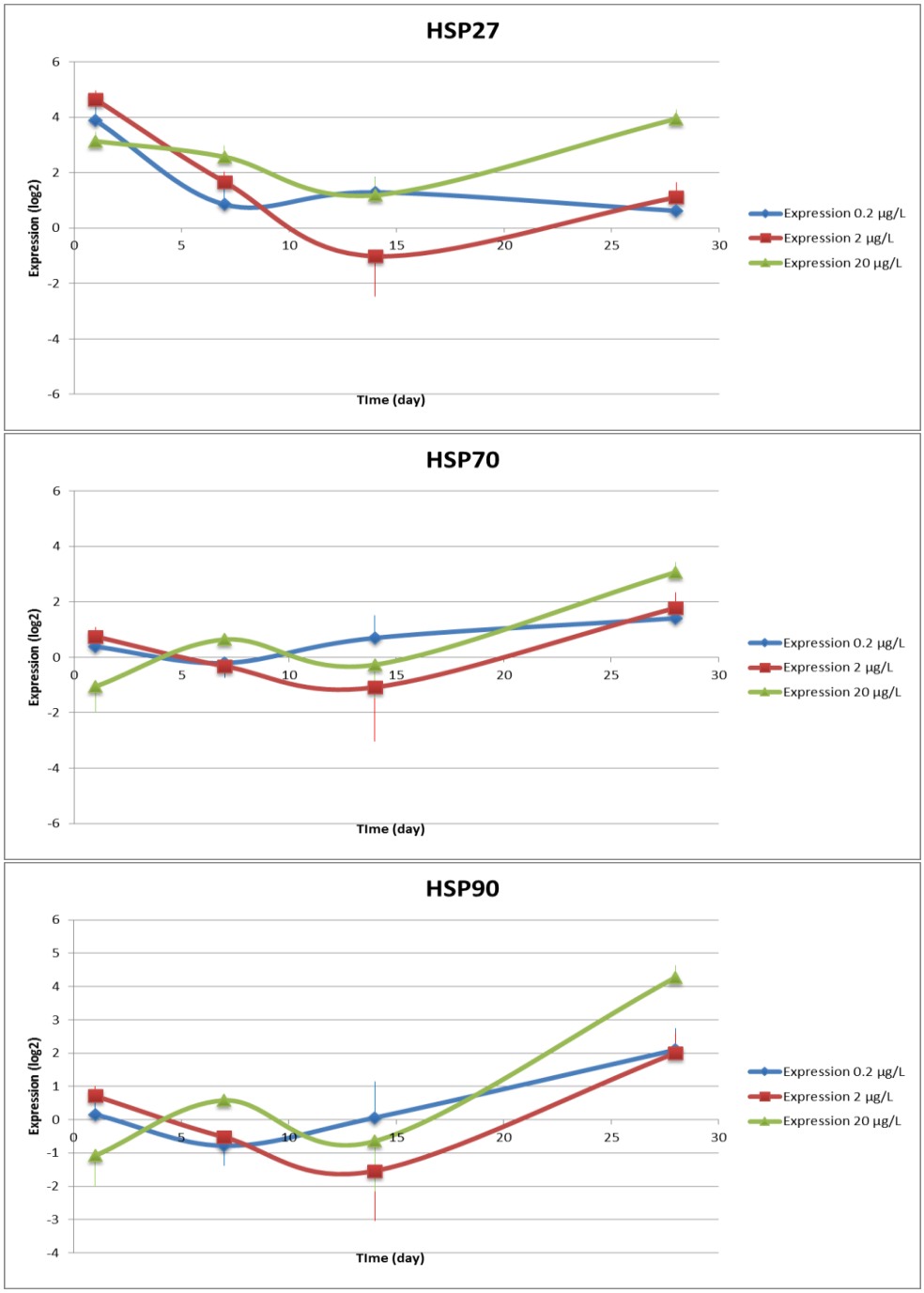

***Fig 35** - Time series analysis of HSPs (relative mRNA levels) in gills of mussels exposed to 5 nm AgENP for 28 days. Shown is the average value ± SEM (n=6) of Ag]exp$_t$/CTRLexp$_t$ at each time (t) and for each AgENP exposure level ([Ag]).*

Biochemical effects of AgENPs.

Metallothionein protein concentration was evaluated in tissues (digestive gland and gills) exposed to 5 nm ENPs, as well as ionic silver (in form of nitrate). To this aim, a robust and sensitive electrophoretic technique based on fluorescence labelling of MTs was used (Viarengo et al., 1997).

Results obtained in the digestive gland are shown in Fig. 36. Ionic silver was unable to stimulate MT protein accumulation. From the density distribution plot, instead, it is arguable a modest yet significant shift of MT content data distribution for what concerns the ENP treated samples (Kolmogorov-Smirnov two sample test, $p<0.0001$). In 2 µg/L AgENPs treated specimens this difference was driven by samples (2 out 8) showing an additional MT band below 20 kda in the electropherogram (Fig. 36, panel B). This protein is compatible with the MT20 gene product that as previously explained represents the xenobiotic metal inducible form.

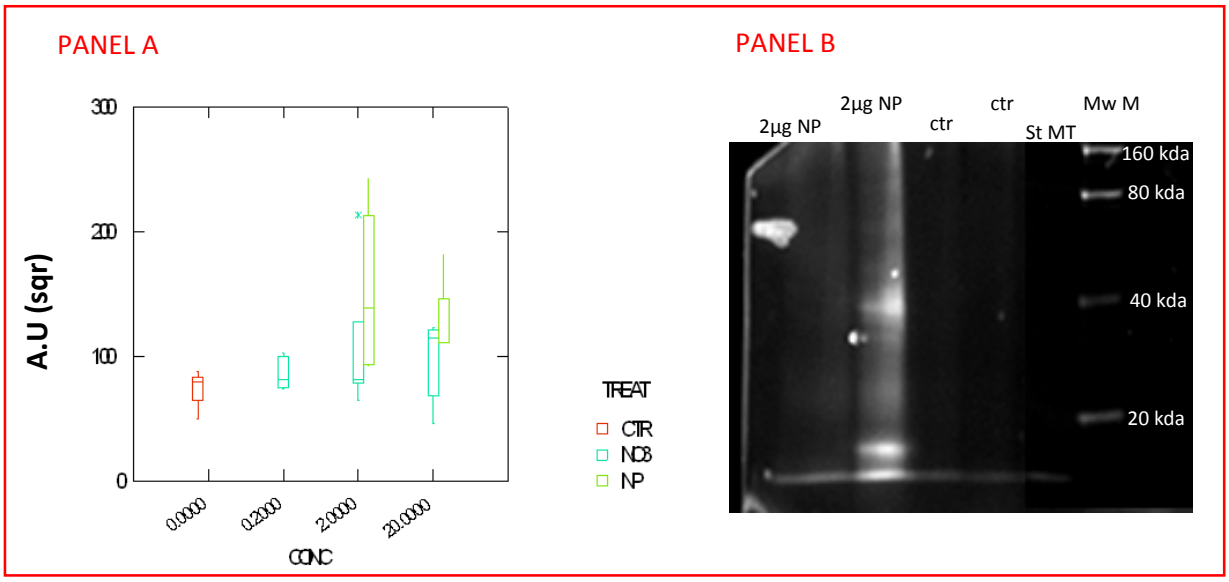

***Fig 36** - **Panel A**. Digestive gland MT content (density distribution). Box plot display the square root (sqr) transformation of the integrated density evaluated from image analysis of SDS-PAGE. The average MT content in control digestive gland was 4.6 µg /mg protein in the S30 supernatant. MT content was not evaluated in the 0.2 µg/L ENP samples. Difference from control Kruskall-wallis test statistics, p< 0.1 n=10.*

***Panel B**. Representative 12% Tris-Glycine SDS PAGE showing the additional MT band in the digestive gland of NP treated mussels. Prior to electrophoresis, mussel MT were partially purified by ethanol fractionation (from equal amount of proteins) and labelled with a UV-fluorescent dye for sulphydrils. Rabbit liver purified MT (50 ng) was used as a qualitative/quantitative standard.*

The MT content in gills is depicted in Fig. 37. In this case, two samples Kolmogorov-Smirnov statistics showed differences between control not exposed specimens and either silver forms ($p < 0.01$ for nitrate; p0=0.08 for ENPs), and differences between $AgNO_3$ and AgENPs ($p < 0.05$). These results strongly support our previously addressed hypothesis that ENPs effects/toxicity arise from the combination of an externally dissolved silver fraction acting through the gills and a ENP derived one acting more specifically through the digestive gland.

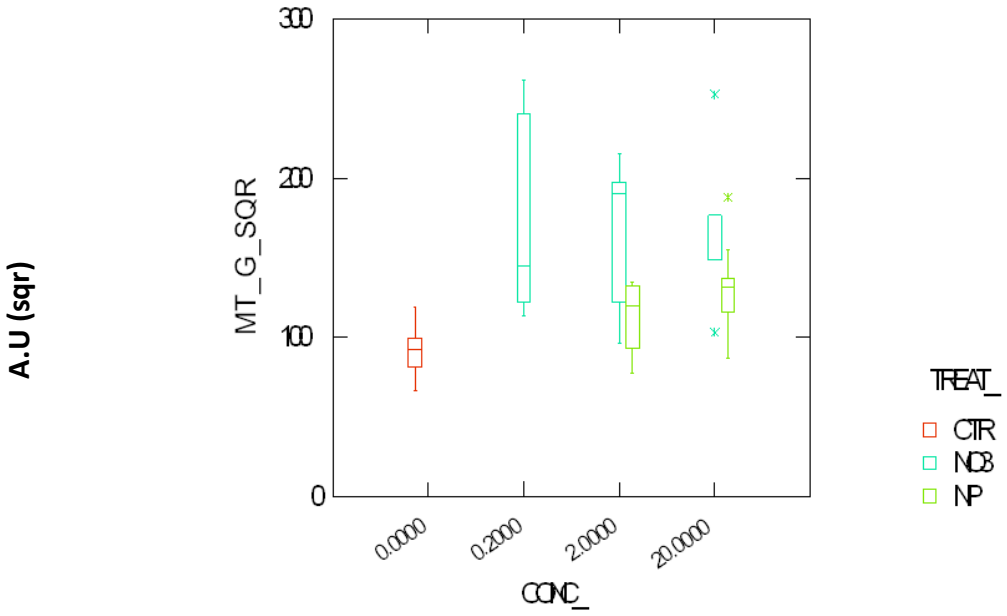

***Fig 37** - Gill MT content (density distribution). Box plot display the square root (sqr) transformation of the integrated density evaluated from image analysis of SDS-PAGE. The average MT content in control gills was 5.2 µg /mg protein in the S30 supernatant. MT content was not evaluated in the 0.2 µg/L ENP samples*

To get further clues in the toxicity route of silver and AgENPs we looked at biochemical activities of antioxidant enzymes in either tissue. Catalase, superoxide dismutase and glutathione-peroxidase activities were analysed by means of in gel assays (Weydert and Cullen, 2010). For CAT and SOD very similar patterns were observed for the effects of silver nitrate that, in general, increased enzyme activities in both tissues. In the digestive gland, these effects appeared limited to a fixed threshold, whilst in gills there was a smoothed dose dependent effect (Fig 38 and 39). GPX activity increased only in gills for the effects of silver

nitrate at 20 µg/L (data not shown). Activation of CAT and SOD activities have been often associated to moderate oxidative stress syndrome and increased heavy metal loads in mussel tissues, in particular digestive gland but also gills (Vlahogianni et al., 2007).

The effects of AgENP were very different from those of ionic silver since CAT -and to a lesser

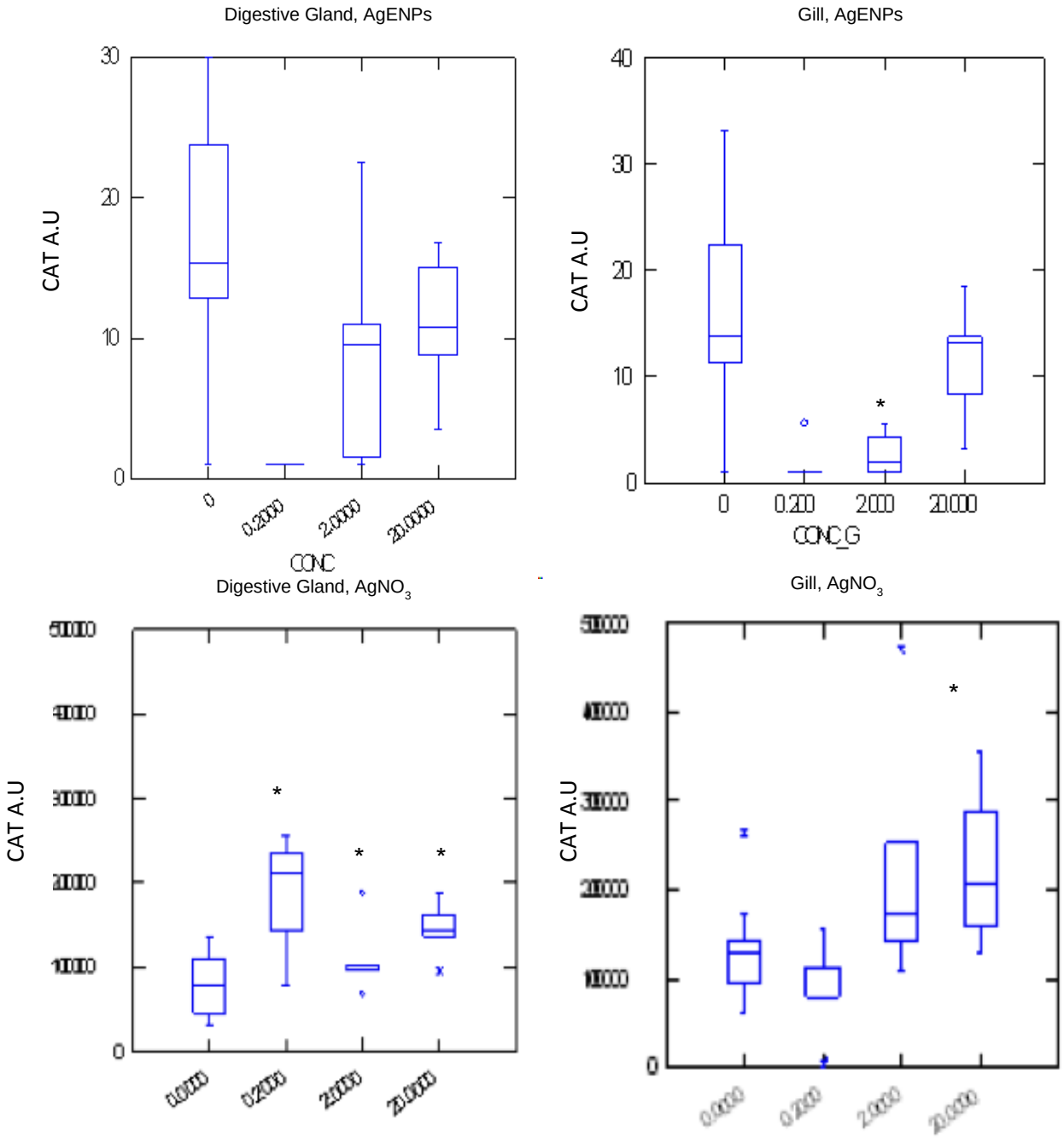

*Fig 38 - Enzymatic activity of Catalase in tissues of mussels exposed to $AgNO_3$ and 5 nm AgENP for 28 days. Shown is the box plot of densitometric analysis obtained from in gel assay (n=8). Catalase activity is expressed in arbitrary units. * statistically different from control (0.000) condition. P < 0.05 ; ° p < 0.1, according to 2 samples Kolmogorov-Smirnov test statistics. Data for 0.2 µg/L ENPs were not collected.*

extent SOD- have displayed a trend of inhibition. Other authors reported a fair increase of CAT and SOD activity for the effects of CuO ENPs in the digestive gland, along with increased membrane lipid peroxidation byproducts (Gomes et al., 2012). Also silica and titania ENPs increased CAT activity in same tissue (Canesi et al., 2010). In the digestive gland of *Lymnea*

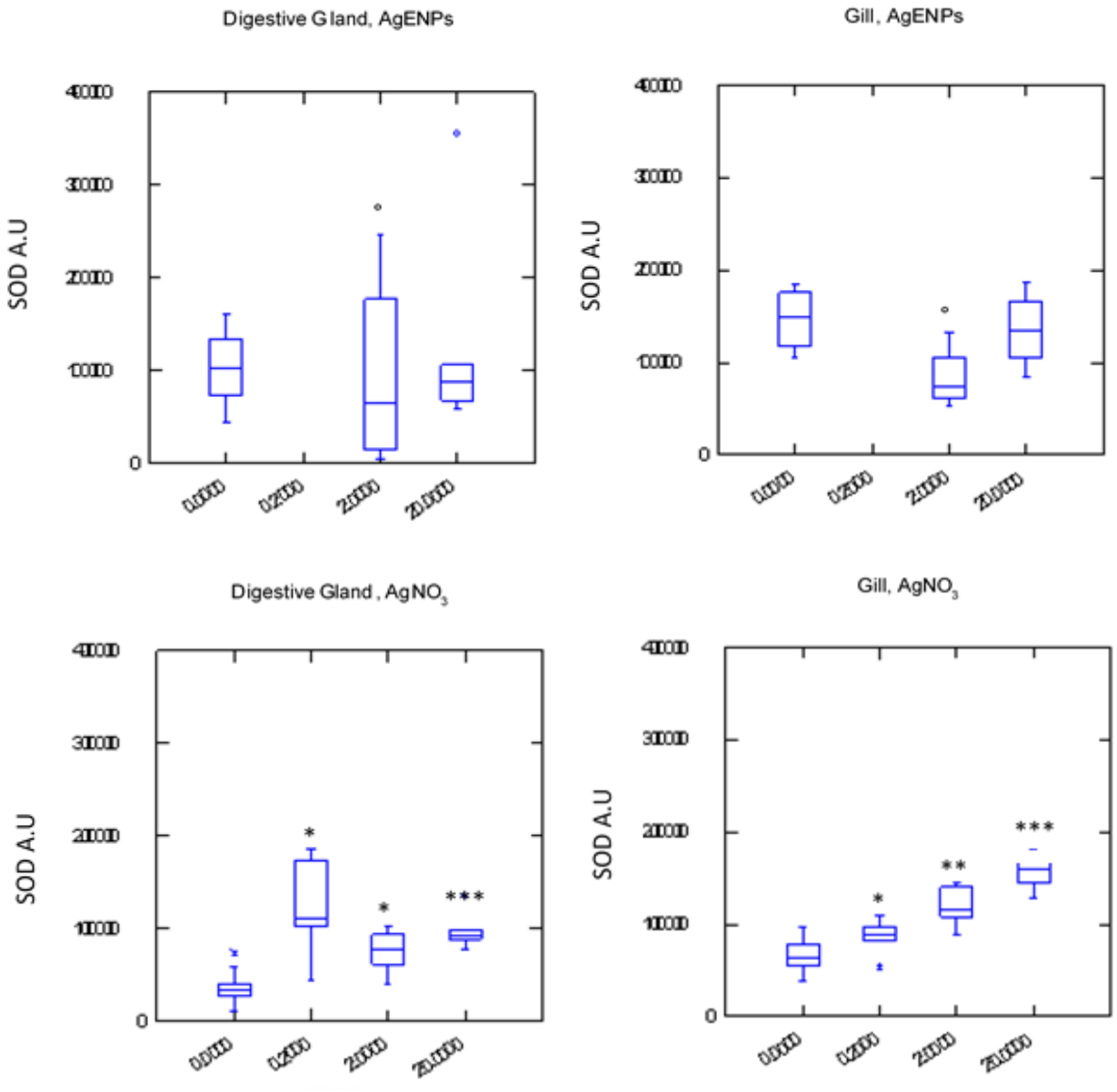

Fig 39* - Enzymatic activity of superoxide dismutase in tissues of mussels exposed to $AgNO_3$ and 5 nm AgENP for 28 days.
Shown is the box plot of densitometric analysis obtained from in gel assay (n=8)
SOD activity is expressed in arbitrary units. *** statistically different from control (0.000) condition, P < 0.001 ; **, p<0.01; * p<0.05; ° p < 0.1, according to 2 samples Kolmogorov-Smirnov test statistics.
Data for 0.2 µg/L ENPs were not collected.

luteola, a pulmonate freshwater snail, AgENP increased CAT activity and lipid membrane peroxidation byproducts, even if other antioxidant enzymes such as gpx and glutathione reductase decreased (Ali et al., 2013). Ag ENP induced cat activity and oxidative stress also in mammalian systems, such as human lung epithelial (A549) cells (Suliman et al., 2013).

This complex of data is in contrast with our results that instead showed a moderate inhibition of cat. However, it should be underlined that silver is among the strongest enzymatic inhibitor of catalase in fish (*Fundulus heteroclitus*) tissues (Jackim et al., 1970) and moreover, a direct interaction of AgENP to catalase has been demonstrated by *in silico* structural studies (Gavanji et al., 2013). Therefore results observed in the digestive gland for the 5 nm AgENPs are not controversial and yet seem to suggest a different mode of action for ENP derived bio-accumulated silver. It can be argued that AgENP enters digestive gland selectively, most likely not in the original nano-sized form (see Chapter 2 and Appendix). Once into the tissue, it can oxidize to Ag^{+} behaving as a potent electrophilic cation. Moreover, elemental silver can catalyze the oxidation by atomic oxygen that adsorbs on its metallic surface. Atomic oxygen instantaneously oxidizes organic material on contact, including reduced cysteines to sulfhydryl-bridged bonds (Davies and Etris, 1997). It is not the aim of this work to speculate on those arguments, but to elucidate the biological damage arising from the uptake of colloidal silver into mussel tissues.

To this end, we looked to oxidative damage in the digestive gland by means of a well characterized histochemical approached, i.e. lipofuscin granule accumulation. Lipofuscin are byproducts of lipid membrane peroxidation, an oxidative process usually promoted by heavy metals in mussel tissues (Viarengo et al., 2007). The significant accumulation of lipofuscin granules in the digestive gland of specimens exposed to 20 µg/L AgENP indicates the occurrence of oxidative stress related processes for the effects of colloidal silver (Fig. 40).

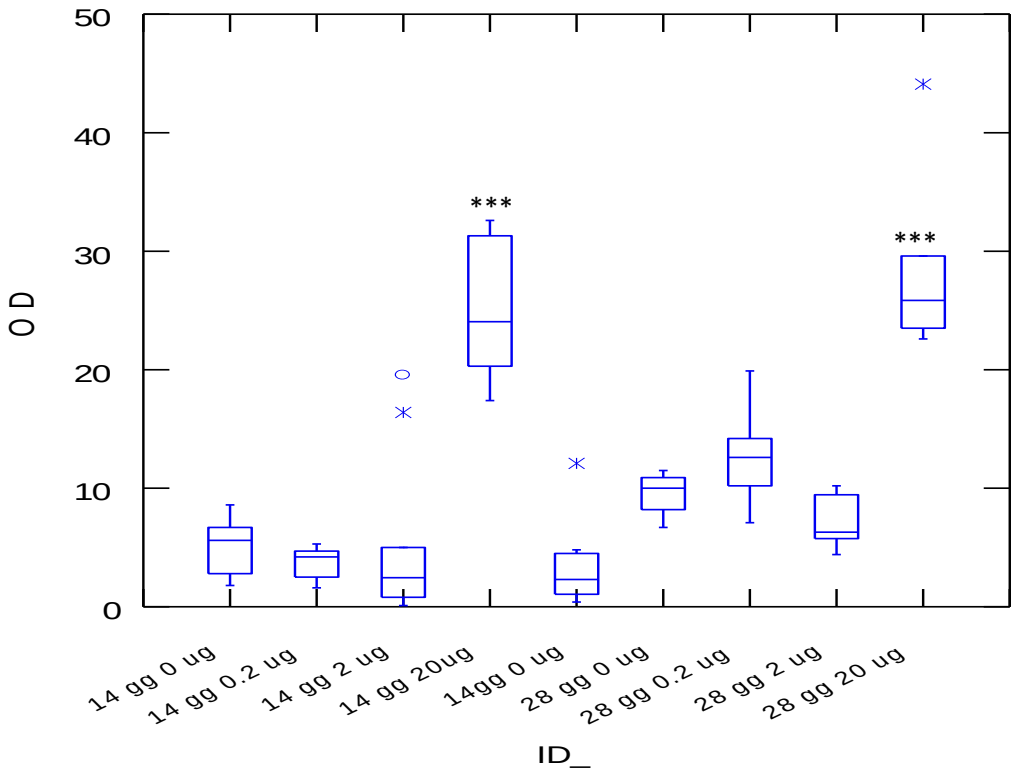

***Fig 40** - Lipofuscin accumulation in mussel digestive gland*
Shown is the box plot of densitometric analysis obtained from 10 transversal 10 µm tissue sections (n=10).
Optical density (OD) is expressed in arbitrary units.
Data are shown for day 14 and day 28 of exposure to 5 nm AgENPs.
****** statistically different from control condition at time t, P < 0.0001; according to 2 samples Kolmogorov-Smirnov test statistics.***

Cellular oxidative damage not only affects lipids, but also DNA and proteins (Stadtman et al,. 1992). Protein carbonylation is an irreversible oxidative modification of proteins that is widely used to infer the occurrence of oxidative stress in cellular system.

Furthermore, carbonyl modifications can be produced by wide variety of ROS as well as by-products of lipid oxidation (LJ Yan and Forster, 2012). Another advantage of studying protein carbonyl modification is that is can be measured in different tissues using the same biochemical approach based on protein western-blot and immunological detection with a specific antibody after derivatization of protein with 2, 4-dinitrophenylhydazine (DNPH) (reviewed in LJ Yan and Forster, 2012). To dissect the effects of soluble and colloidal silver, carbonylated cytosolic proteins were investigated in digestive gland and gills in specimens

exposed to either form of silver. Results obtained in the digestive gland are shown in Fig. 41. Indeed, AgENPs elicited a dose dependent increase of protein oxidation, whilst nitrate was unable to produce any reproducible effects. Conversely, carbonylated proteins found in gills for the effects of AgENP exposure or silver nitrate showed consistent overlaps (Fig. 42). First, these data confirmed that silver elicit oxidative damage whatever its form. Second, this result is another confirmation that AgENPs act through a bimodal action mode driven by soluble silver in gills and colloidal in the digestive gland.

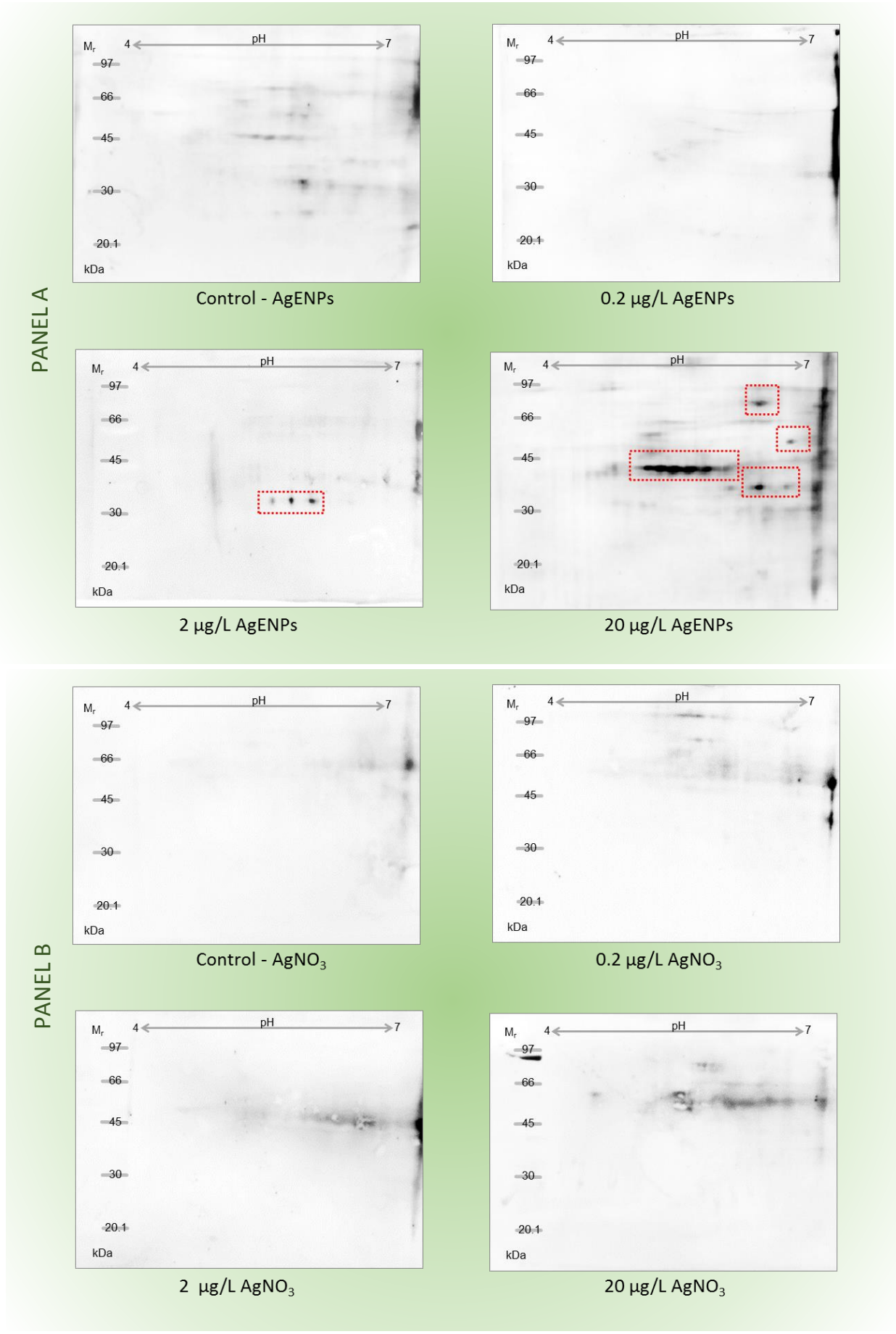

***Fig 41** - Immunochemical determination of carbonylated proteins in the digestive gland of mussels (2DE western-blot)*

Shown are carbonylatated citosolic proteins derivatized with 2,4-dinitrophenylhydrazine (DNPH), separated by bi-dimensional electrophoresis and further stained with an anti-DNP antibody from 2DE western blot. Red box indicate protein with increased carbonylation signal with respect to control.

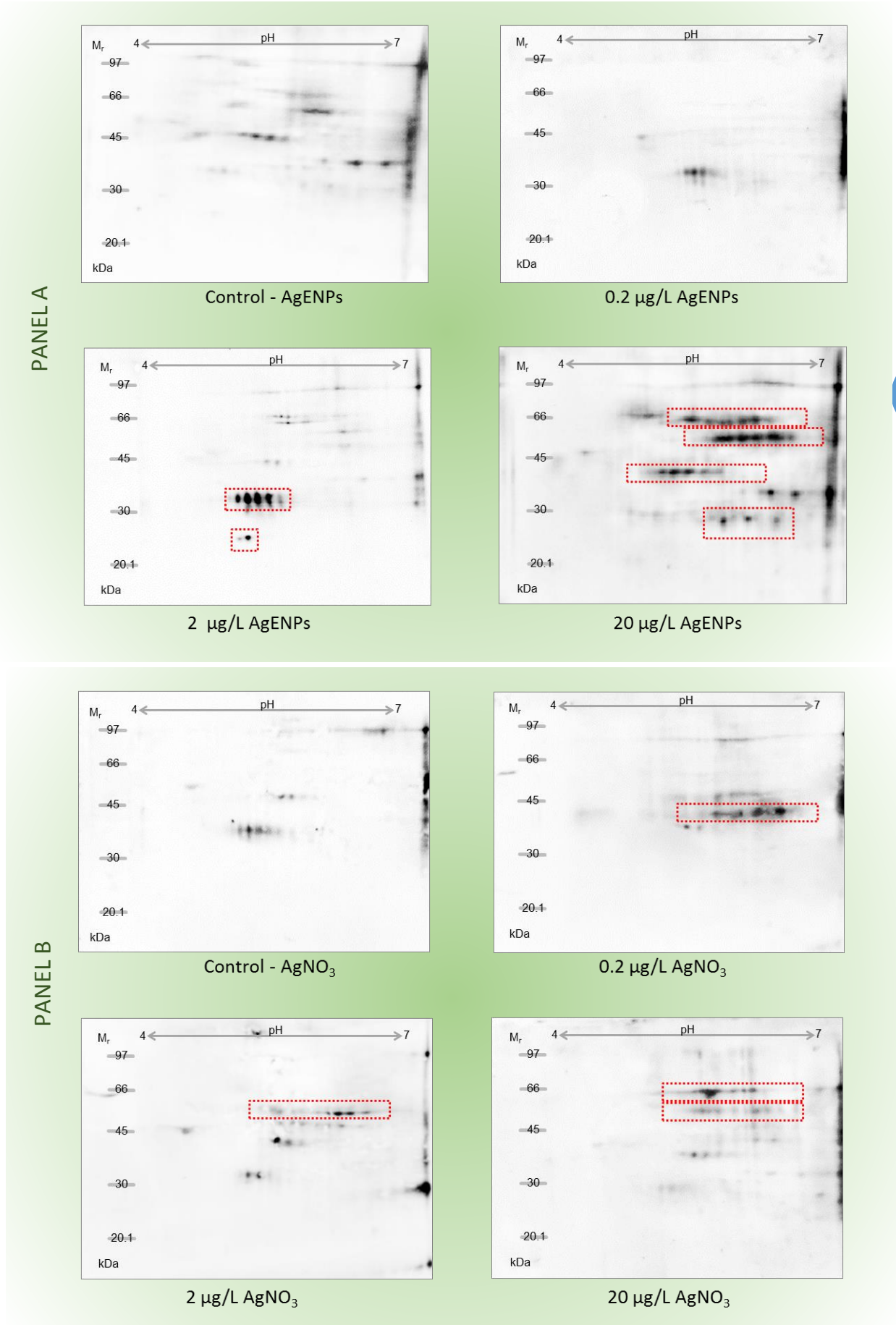

***Fig 42** - Immunochemical determination of carbonylated proteins in the gills of mussels (2DE western-blot) Shown are carbonylatated citosolic proteins derivatized with 2,4-dinitrophenylhydrazine (DNPH), separated by bi-dimensional electrophoresis and further stained with an anti-DNP antibody from 2DE western blot. Red box indicate protein with increased carbonylation signal with respect to control.*